Acta Pharmacologica Sinica (2018) 39: 357–370
 1671-4083/18
www.nature.com/aps

Article

Barbaloin inhibits ventricular arrhythmias in rabbits by modulating voltage-gated ion channels

Zhen-zhen CAO#, You-jia TIAN#, Jie HAO#, Pei-hua ZHANG, Zhi-pei LIU, Wan-zhen JIANG, Meng-liu ZENG, Pei-pei ZHANG, Ji-hua MA*

The Cardio-Electrophysiological Research Laboratory, Medical College, Wuhan University of Science and Technology, Wuhan 430065, China

Abstract

Barbaloin (10-β-*D*-glucopyranosyl-1,8-dihydroxy-3-(hydroxymethyl)-9(10H)-anthracenone) is extracted from the aloe plant and has been reported to have anti-inflammatory, antitumor, antibacterial, and other biological activities. Here, we investigated the effects of barbaloin on cardiac electrophysiology, which has not been reported thus far. Cardiac action potentials (APs) and ionic currents were recorded in isolated rabbit ventricular myocytes using whole-cell patch-clamp technique. Additionally, the antiarrhythmic effect of barbaloin was examined in Langendorff-perfused rabbit hearts. In current-clamp recording, application of barbaloin (100 and 200 μmol/L) dose-dependently reduced the action potential duration (APD) and the maximum depolarization velocity (V_{max}), and attenuated APD reverse-rate dependence (RRD) in ventricular myocytes. Furthermore, barbaloin (100 and 200 μmol/L) effectively eliminated ATX II-induced early afterdepolarizations (EADs) and Ca^{2+}-induced delayed afterdepolarizations (DADs) in ventricular myocytes. In voltage-clamp recording, barbaloin (10–200 μmol/L) dose-dependently inhibited L-type calcium current ($I_{Ca.L}$) and peak sodium current ($I_{Na.P}$) with IC_{50} values of 137.06 and 559.80 μmol/L, respectively. Application of barbaloin (100, 200 μmol/L) decreased ATX II-enhanced late sodium current ($I_{Na.L}$) by 36.6%±3.3% and 71.8%±6.5%, respectively. However, barbaloin up to 800 μmol/L did not affect the inward rectifier potassium current (I_{K1}) or the rapidly activated delayed rectifier potassium current (I_{Kr}) in ventricular myocytes. In Langendorff-perfused rabbit hearts, barbaloin (200 μmol/L) significantly inhibited aconitine-induced ventricular arrhythmias. These results demonstrate that barbaloin has potential as an antiarrhythmic drug.

Keywords: arrhythmias; aloe; barbaloin; ventricular myocytes; late sodium current; peak sodium current; L-type calcium current; afterdepolarization; ATX II; aconitine

Acta Pharmacologica Sinica (2018) 39: 357–370; doi: 10.1038/aps.2017.93; published online 26 Oct 2017

Introduction

Researchers have conducted intensive studies to explore the potential therapeutic effects of various foods and natural herbal plants on diseases. Aloe, a perennial liliaceous natural herbal plant,has been used in folk medicine for centuries[1]. Currently, aloe vera gel is sold commercially worldwide and is used as an ingredient in a wide range of food, cosmetic and therapeutic products[2]. It has recently been reported that incorporating aloe vera gel into emulsion-based goat meat nuggets enriches the functional value of the product[3]. Barbaloin (10-beta-*D*-glucopyranosyl-1,8-dihydroxy-3-(hydroxymethyl)-9(10H)-anthracenone) is considered the most specific extract of aloe[4] and has been reported to have a variety of pharmacological effects, including anti-inflammatory, antiviral, antibacterial, antitumor and free radical-scavenging effects[4-9]. Moreover, Lam *et al* have found that barbaloin protects low-density lipoproteins and erythrocytes from oxidative damage, thus indicating that the compound may have potential as a therapy for important cardiovascular diseases[10]. Thus, we surmised that barbaloin might protect the heart from arrhythmia-related cardiac disorders, a topic has not previously been investigated.

Cardiac arrhythmias, which are attributed to the dysfunction of the cardiac pacemaking and conduction systems, comprise a group of severe diseases and are associated with many life-threatening conditions, such as heart failure and sudden cardiac death[11, 12]. Therefore, studies to identify drugs that may be used for the treatment of cardiac arrhythmia are urgently needed. Heart arrhythmias develop when cardiac electrical activity becomes dysfunctional[13]. Cardiac electrical activity is determined by the generation and propagation of myocardial

# These authors contributed equally to this work.
*To whom correspondence should be addressed.
E-mail mjhua@wust.edu.cn
Received 2017-02-28 Accepted 2017-06-17

action potentials (APs) through various transmembrane ionic currents[14].

From the above reports, we hypothesized that barbaloin might have cardioprotective effects. Therefore, in the present study, we examined the effects of barbaloin on APs, as well as on early afterdepolarizations (EADs) and delayed afterdepolarizations (DADs), in ventricular myocytes to explore its potential antiarrhythmic effects. Additionally, we performed experiments to investigate how barbaloin affects transmembrane ionic currents, including L-type calcium current ($I_{Ca.L}$), late sodium current ($I_{Na.L}$), peak sodium current ($I_{Na.P}$), inward rectifier potassium current (I_{K1})and rapidlyactivateddelayed rectifier potassium current(I_{Kr}). To test our hypothesis, the effects of barbaloin on Langendorff-perfused rabbit hearts were also examined.

Materials and methods

Isolation of ventricular myocytes

The animal experiments performed in this investigation were approved by the Institutional Animal Care and Use Committee of Wuhan University of Science and Technology and complied with the ethical standards outlined in the Guide for the Care and Use of Laboratory Animals (National Institutes of Health, publication No 85-23). Adult New Zealand white rabbits of either sex weighing 1.5–2 kg were anesthetized with ketamine (Fujian Gutian Pharmaceutical Co, Ltd, Gutian, Fujian, China, 30 mg/kg, iv) and xylazine (Shanghai Shifeng Biological Technology Co, Ltd, Shanghai, China, 7.5 mg/kg, im) 20 min after being treated with heparin (2000 U). After the corneal reflex of each rabbit had disappeared, we isolated ventricular myocytes from the rabbits by using the procedure detailed below. First, we placed the rabbits in a fixed position and immediately performed a thoracotomy to remove their hearts, which were placed in a Petri dish filled with Ca^{2+}-free Tyrode's solution containing the following compounds (in mmol/L): NaCl 135, KCl 5.4, $MgCl_2$ 1, NaH_2PO_4 0.33, HEPES 10, and glucose 10 (pH adjusted to 7.4 with NaOH). Then, we removed the fat and connective tissue from each heart, cannulated the aorta, and used a modified Langendorff apparatus to retrogradely perfuse the heart with Ca^{2+}-free Tyrode's solution for 5 min to eliminate residual blood in the heart cavity. Subsequently, we perfused the heart with Ca^{2+}-free Tyrode's solution containing collagenase (type I, 1 mg/mL) and BSA (1 mg/mL) for approximately 40 min. Then, we perfused the heart with KB solution containing (in mmol/L) KOH 70, KCl 40, KH_2PO_4 20, $MgCl_2$ 1, taurine 20, glutamic acid 50, EGTA 0.5, HEPES 10, glucose 10, and HEPES 10 (pH adjusted to 7.4 with KOH) with BSA (1 mg/mL) for an additional 5 min before cutting the left ventricle into small chunks. We obtained single ventricular myocytes by filtering the chunks through a nylon mesh and stored the cells in KB solution containing BSA (1 mg/mL). All perfusates used during this process were bubbled with 95% O_2 and 5% CO_2 and were maintained at 37 °C.

Solutions and drugs

A pipette solution containing the following compounds was used to record APs (in mmol/L): NaCl 5, KCl 30, K-aspartate 110, creatine phosphate 5, Mg-ATP 5, EGTA 0.1, HEPES 10, and cAMP 0.05 (pH adjusted to 7.3 with KOH). The bath solution contained the following (in mmol/L): NaCl 145, KCl 5.4, $CaCl_2$ 1.8, $MgCl_2$ 1.2, HEPES 5, and glucose 10 (pH adjusted to 7.4 with NaOH).

A pipette solution containing the following compounds was used to record $I_{Ca.L}$ and $I_{Na.L}$ (in mmol/L): CsCl 120, $CaCl_2$ 1, $MgCl_2$ 5, Na_2ATP 5, TEACl 10, EGTA 11, and HEPES 10 (pH adjusted to 7.3 with CsOH). The bath solution contained the following compounds (in mmol/L): NaCl 135, CsCl 5.4, $CaCl_2$ 1.8, $MgCl_2$ 1, $BaCl_2$ 0.3, NaH_2PO_4 0.33, HEPES 10, and glucose 10 (pH adjusted to 7.4 with NaOH). We added 10 μmol/L nifedipine to the extracellular solution to block $I_{Ca.L}$ during $I_{Na.L}$ recording.

A bath solution containing the following compounds was used to record $I_{Na.P}$ (in mmol/L): NaCl 30, $CsCl_2$ 105, $CaCl_2$ 1, $MgCl_2$ 1, $CdCl_2$ 0.05, HEPES 10, and glucose 10 (pH adjusted to 7.4 with CsOH). The pipette solution used for $I_{Na.P}$ recording was identical to that used for $I_{Ca.L}$ and $I_{Na.L}$ recording.

A pipette solution containing the following compounds was used to record I_{Kr} and I_{K1} (in mmol/L): KCl 20, $MgCl_2$ 1, K-aspartate 110, Na_2-phosphocreatine 5, GTP 0.1, Mg-ATP 5, EGTA 5, and HEPES 10 (pH adjusted to 7.3 with KOH). The bath solution contained the following compounds (in mmol/L): NaCl 140, KCl 5.4, $CaCl_2$ 1.8, $MgCl_2$ 1, $CdCl_2$ 0.2, NaH_2PO_4 0.33, HEPES 10, and glucose 10 (pH adjusted to 7.4 with NaOH). We added 30 μmol/L chromanol 293B to the extracellular solution to block I_{Ks} during I_{Kr} recording.

CsCl and KH_2PO_4 were purchased from Amresco (Solon, OH, USA), and EGTA and HEPES were obtained from BioSharp (Hefei, China). ATX II and TTX were purchased from the Alomone Labs (Jerusalem, Israel) and Tocris (Ellisville, MO, USA), respectively. BSA was purchased from Roche (Basel, Switzerland), and barbaloin was obtained from Beijing Standard Material Network (Beijing, China), dissolved in methanol and used within 8 h. All other chemicals, including collagenase (type I), were purchased from Sigma-Aldrich Co (St Louis, MO, USA).

Cellular electrophysiological recording

The bath solutions were maintained at 37 °C and bubbled with 95% O_2 and 5% CO_2 throughout the experiment. The isolated ventricular myocytes were sedimented in a cell chamber with a 1 mL volume and were mounted on the stage of an inverted microscope for 10 min before being superfused with the appropriate oxygenized bath solution at a rate of 2 mL/min. Glass electrodes with resistances ranging from 1 to 3 MΩ were pulled with a two-stage puller (PP-830, Narishige Group, Tokyo, Japan) after being filled with pipette solution. Only rod-shaped myocytes showing clear striations were selected for sealing. Their cell membranes were subsequently ruptured by pulsed negative suction to form the whole-cell configuration. Membrane capacitance and series resistance were compensated for to obtain minimal contributions from the capacitive transients.

For the AP recordings, we switched the recording mode from whole-cell clamp mode to current-clamp mode after forming the whole-cell configuration. We elicited the APs by continuously stimulating the cells with 6-ms pulses that were 1.5-fold greater than the threshold for different cycle lengths (CLs).

For the $I_{Ca.L}$ recordings, we used a holding potential of -40 mV. The currents used for the current-voltage (*I–V*) relationship studies were elicited by 300-ms depolarizing pulses from -40 mV to +55 mV in 5-mV increments. The steady-state inactivation protocol comprised 2-s depolarizing prepulses from -50 mV to 0 mV in 5-mV increments, which was followed by a 300-ms test pulse of 0 mV.

For the $I_{Na.P}$ and $I_{Na.L}$ recordings, we used a holding potential of -90 mV. The currents used for the $I_{Na.P}$ and $I_{Na.L}$ *I-V* relationship studies were elicited by 300-ms depolarizing pulses from -70 mV to +40 mV in 5-mV increments and from -80 mV to +60 mV in 10-mV increments, respectively. Single $I_{Na.L}$ recordings were obtained by depolarizing the cells to -20 mV from the holding potential. The $I_{Na.P}$ steady-state inactivation protocol comprised 100-ms depolarizing prepulses from -110 mV to -50 mV in 5-mV increments, which was followed by a 100-ms test pulse of -30 mV.

For the I_{Kr} and I_{K1} recordings, we used a holding potential of -40 mV. I_{Kr} was elicited by depolarizing pulses from -40 mV to +50 mV in 10-mV increments for 3 s and then returning to -40 mV for 5 s, whereas I_{K1} was elicited by pulses that were initially hyperpolarizing and then depolarizing from -120 mV to +50 mV in 10-mV increments for 400 ms.

All the electrophysiological recordings were obtained with an EPC 10 amplifier (HEKA Electronic, Lambrecht, Germany), filtered at 2 kHz, digitized at 10 kHz and then stored on a computer hard disk for further analysis.

Electrocardiogram (ECG) recordings of Langendorff-perfused rabbit hearts

The rabbit hearts used in the present experiments were excised as described above. The hearts were then rapidly cannulated in the aortas and perfused with normal Tyrode's solution with a Langendorff apparatus for 15 min before ECG recordings. All of the Tyrode's solution used in the present experiments was maintained at 37 °C and bubbled with 95% O_2 and 5% CO_2. Hearts that did not exhibit a regular spontaneous rhythm or that had irreversible myocardial ischemia were excluded from analysis. The ECG recordings were divided into the following four groups: a control group, a barbaloin-treated group, an aconitine-treated group, and a barbaloin and aconitine co-treatment group. The rabbit hearts were recorded for 90 min in all groups. The hearts were perfused with normal Tyrode's solution throughout the experiments in the control group, whereas the hearts in the barbaloin-treated and aconitine-treated groups were perfused with normal Tyrode's solution for the first 10 min and 20 min and were then perfused with Tyrode's solution containing 200 μmol/L barbaloin and 100 nmol/L aconitine, respectively, for the remaining time. However, the hearts in the barbaloin and aconitine co-treatment group were first perfused with normal Tyrode's solution for 10 min, then perfused with Tyrode's solution containing 200 μmol/L barbaloin for another 10 min, and finally perfused with Tyrode's solution containing both 200 μmol/L barbaloin and 100 nmol/L aconitine for the remaining time. The ECG recordings of the Langendorff-perfused rabbit hearts were obtained with a BL-420F biological data signal acquisition and analysis system (Techman Software, Chengdu, China).

Data analysis

The currents recorded with the whole-cell configuration were normalized to current density, which was determined by dividing the membrane capacitance, for further analysis. The figures were plotted and fitted with Origin (V7.0, OriginLab, Northampton, MA, USA). The $I_{Ca.L}$ and $I_{Na.P}$ concentration-response curves were fitted with the Hill equation, $Y=B_{max}/[1+(IC_{50}/D)^n]$, where B_{max} is the maximum blockage of currents, IC_{50} is the barbaloin concentration for half-maximum blockage, D is the barbaloin concentration, and n is the Hill coefficient. Y is the percentage of current blocked, which is defined as $(I_{control}-I_{drug})/I_{control}$, where $I_{control}$ and I_{drug} are the current amplitudes before and after barbaloin administration, respectively. The $I_{Ca.L}$ and $I_{Na.P}$ steady-state activation and inactivation curves were fitted with the Boltzmann equation, $Y=1/\{1+\exp[(V_m-V_{1/2})/k]\}$, where V_m is the membrane potential, $V_{1/2}$ is the half-activation or half-inactivation potential, and k is the slope factor. The Y value represents the relative conductance (G/G_{max}) and relative current (I/I_{max}) for the steady-state activation and inactivation curves, respectively. All data were analyzed using FitMaster (v2x32, HEKA) and Origin 7.0 and are expressed as percentage and as the mean±SD. Statistical significance was determined using one-way analysis of variance (ANOVA) followed by Student's *t*-test. $P<0.05$ was considered statistically significant.

Results

Effects of barbaloin on APs

The AP parameters assessed in the present study were the resting membrane potential (RMP), action potential amplitude (APA), maximum depolarization velocity (V_{max}) and action potential duration (APD). Of these, the APD was assessed at the following two different levels: 50% completion of repolarization (APD_{50}) and 90% completion of repolarization (APD_{90}). Barbaloin exerted distinct effects on the different parameters when the APs were continuously recorded at a frequency of 1 Hz (Figure 1B, Table 1). After establishing stable AP recordings, we added 100 and 200 μmol/L barbaloin to the bath solution in succession and found that these additions shortened the APD_{50} and APD_{90} in a concentration-dependent manner without significantly changing the RMP. Specifically, we found that 100 and 200 μmol/L barbaloin shortened the APD_{50} by 8.7%±3.7% and 15.8%±5.0% (n=12, $P<0.01$ *vs* 100 μmol/L barbaloin), respectively, and that 100 and 200 μmol/L barbaloin shortened the APD_{90} by 8.5%±2.2% and 15.5%±3.5%, respectively (n=12, $P<0.01$ *vs* 100 μmol/L barbaloin). The APD_{50}/APD_{90} ratio was 0.907±0.020 in the control group, and

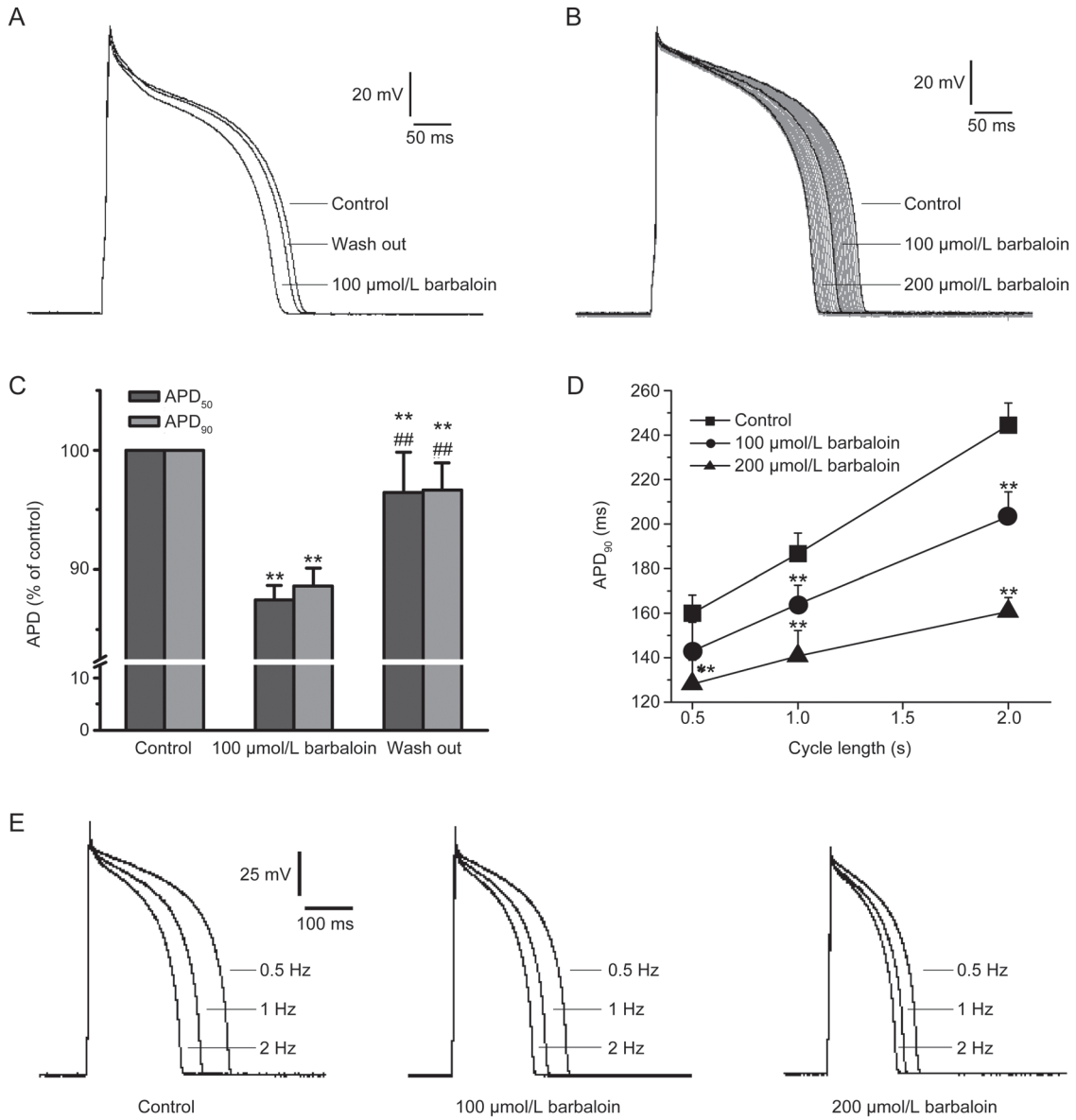

Figure 1. Effects of barbaloin on action potentials (APs) in rabbit ventricular myocytes. (A) Representative traces showing that barbaloin exerted reversible inhibitory effects on APs. (B) Representative traces of APs recorded continuously at a frequency of 1 Hz before (control) and after the administration of 100 and 200 μmol/L barbaloin. The gray traces are the changes in the APs after the administration of barbaloin. (C) Bar graphs showing the mean APD percentage values for the control, 100 μmol/L barbaloin-treated and wash-out groups (n=10. $^{**}P$<0.01 *vs* control. $^{\#\#}P$<0.01 *vs* 100 μmol/L barbaloin). (D) The data for the APD_{90}, which were averaged from 30 sweeps recorded at different cycle lengths (CLs) (n=8. $^{**}P$<0.01 *vs* control). (E) Representative single traces of APs recorded in an alternating manner at frequencies of 0.5, 1 and 2 Hz before (control) and after the administration of 100 and 200 μmol/L barbaloin.

the APD_{50}/APD_{90} ratios were 0.902±0.040 (n=12, P>0.05 *vs* control) and 0.906±0.020 (n=12, P>0.05 *vs* control and 100 μmol/L barbaloin) in the groups treated with 100 and 200 μmol/L barbaloin, respectively. Both barbaloin treatments decreased V_{max} to some extent, but only the decrease in V_{max} elicited by 200 μmol/L barbaloin was statistically significant (Table 1). Moreover, the effects of barbaloin on the APs were reversible (Figure 1A and 1C).

In another group of experiments, we alternated between recording 20 APs at a frequency of 1 Hz and recording experimental APs at different frequencies to eliminate the effects of changes in frequency on the above parameters. We found that 200 μmol/L barbaloin significantly shortened the APD_{90} at frequencies of 0.5, 1 and 2 Hz, whereas 100 μmol/L barbaloin significantly decreased the APD_{90} at all frequencies except 2 Hz (Figure 1D and 1E). We also noted an APD reverse-rate dependence (RRD) in these experiments (Figure 1D and 1C). However, 100 and 200 μmol/L barbaloin decreased the APD_{90} at the frequencies of 0.5, 1 and 2 Hz by 15.1%±3.4%, 12.9%±3.2% (n=8, P>0.05 *vs* 0.5 Hz), and 9.6%±2.5% (n=8,

Table 1. Effects of barbaloin on the parameters of action potential in rabbit ventricular myocytes. n=12. $^{*}P$<0.05, $^{**}P$<0.01 *vs* control. $^{\#\#}P$<0.01 *vs* 100 μmol/L barbaloin.

Parameters	Control	Barbaloin (μmol/L) 100	200
RMP (mV)	87±2	87±3	87±3
APA (mV)	126±8	123±9	120±9
V_{max} (V/s)	208±12	199±15	184±17*
APD_{50} (ms)	218±10	196±13**	167±10$^{\#\#}$
APD_{90} (ms)	238±13	215±11**	184±13$^{\#\#}$

RMP, resting membrane potential; APA, action potential amplitude; V_{max}, maximum depolarization velocity; APD_{50}, action potential duration at 50% completion of repolarization; APD_{90}, action potential duration at 90% completion of repolarization.

P>0.05 *vs* 1 Hz and P<0.05 *vs* 0.5 Hz) and by 29.8%±5.4%, 22.4%±3.9% (n=8, P<0.05 *vs* 0.5 Hz), and 17.8%±3.6% (n=8, P>0.05 *vs* 1 Hz and P<0.01 *vs* 0.5 Hz), respectively, thus indicating that barbaloin attenuated the APD RRD.

Effects of barbaloin on ATX II-induced APD prolongation and EADs, as well as Ca^{2+}-induced DADs

It has been reported that enhanced $I_{Na.L}$ causes APD prolongation and EADs in various pathological conditions[15, 16]. ATX II, an $I_{Na.L}$ opener, significantly enhanced $I_{Na.L}$ and thus significantly increased the incidence of APD prolongation and EADs in the ventricular myocytes (Figure 2A and 2C). To investigate the effects of barbaloin on ATX II-induced APD prolongation and EADs, we obtained two groups of AP recordings at a stimulation frequency of 0.25 Hz. We found that 10 nmol/L ATX II prolonged the APD_{90} from 211±16 ms to 1129±65 ms and induced EADs in 8 of 8 ventricular myocytes (n=9, P<0.01 *vs* control; Figure 2A and 2C). We also found that 100 μmol/L barbaloin and 200 μmol/L barbaloin decreased the APD_{90} from 1129±65 ms to 602±41 and 389±22 ms, respectively. Moreover, 100 μmol/L barbaloin eliminated EADs in 7 of 9 ventricular myocytes, whereas 200 μmol/L barbaloin completely eliminated all 9 of the above-mentioned EADs (n=9, P<0.01 *vs* 10 nmol/L ATX II and 100 μmol/L barbaloin; Figure 2A, 2D and 2E). When the barbaloin was washed out by perfusion with the bath solution containing 10 nmol/L ATX II, the APD_{90} increased to 988±47 ms, and EADs returned in all 9 ventricular myocytes (n=9, P<0.01 *vs* 100 μmol/L barbaloin and 200 μmol/L barbaloin; Figure 2A and 2F).

Barbaloin also abolished Ca^{2+}-induced DADs (Figure 3). As mentioned above, we used an extracellular Ca^{2+} concentration ($[Ca^{2+}]_o$) of 1.8 mmol/L for the AP recordings. When we increased the $[Ca^{2+}]_o$ to 3.6 mmol/L, DADs occurred in 9 of 9 ventricular myocytes after 10 consecutive APs that were recorded at a high frequency of 5 Hz (Figure 3B). However, 100 μmol/L barbaloin eliminated DADs in 7 of 9 ventricular myocytes, whereas 200 μmol/L barbaloin completely eliminated all 9 of the above-mentioned DADs (Figure 3C and 3D). When the barbaloin was washed out by perfusion with the bath solution containing 3.6 mmol/L $CaCl_2$, the DADs returned in all 9 ventricular myocytes (Figure 3E and 3F).

Effects of barbaloin on $I_{Ca.L}$

The run-down phenomenon is an important problem that may

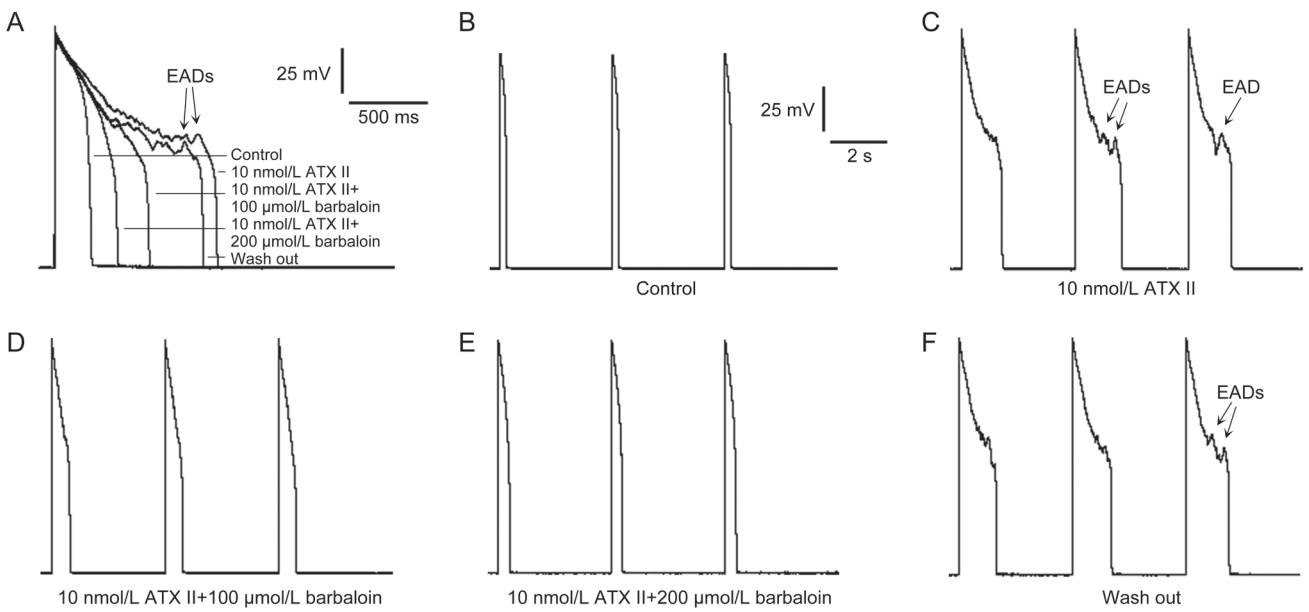

Figure 2. Barbaloin suppressed ATX II-induced early afterdepolarizations (EADs) and action potential duration (APD) prolongation in rabbit ventricular myocytes. (A) Representative single APs recorded at a stimulation frequency of 0.25 Hz. (B, C, D, E and F) show representative traces from the groups subjected to control, 10 nmol/L ATX II, 10 nmol/L ATX II and 100 μmol/L barbaloin, 10 nmol/L ATX II and 200 μmol/L barbaloin and wash-out treatment, respectively. These 3 consecutive APs were recorded at a stimulation frequency of 0.25 Hz with a CL of 12.5 s.

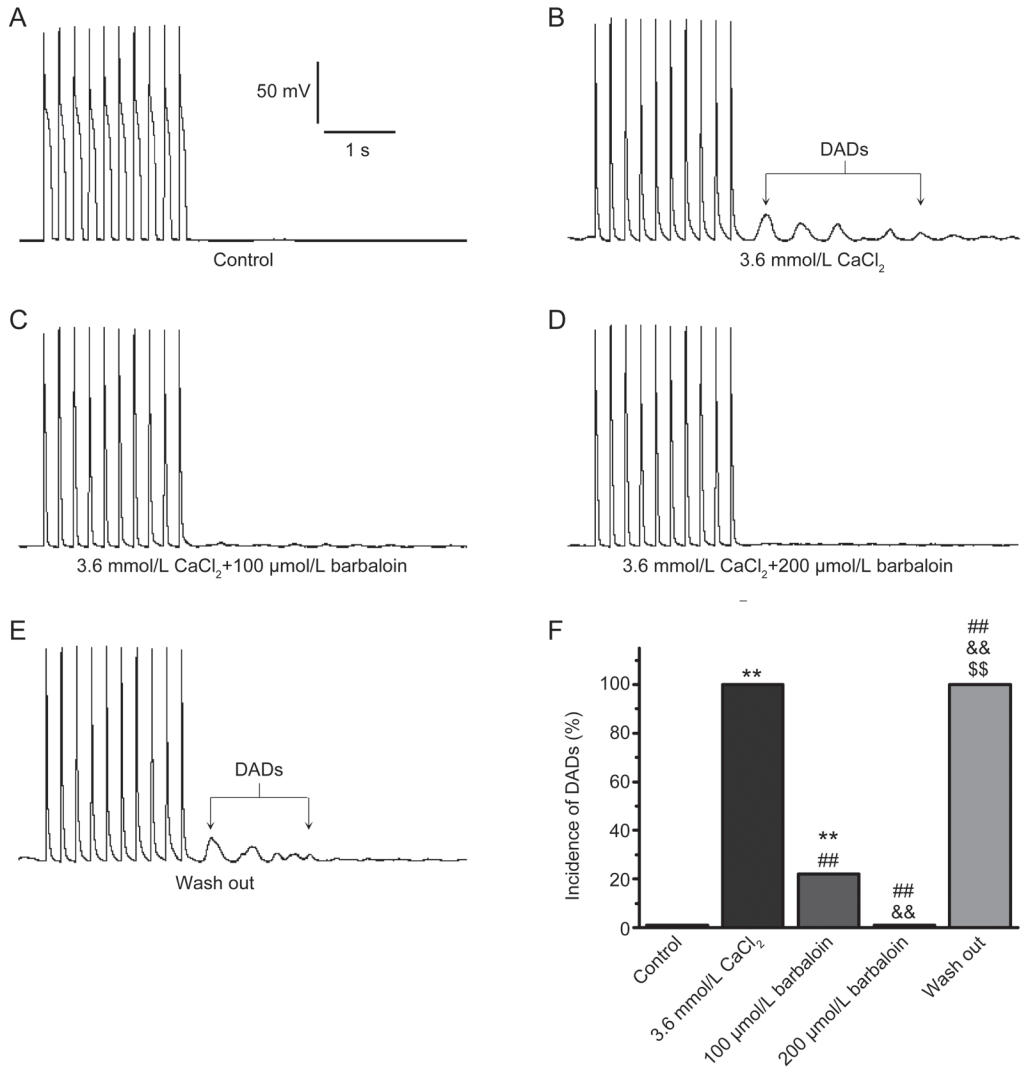

Figure 3. Barbaloin suppressed delayed afterdepolarizations (DADs) induced by the extracellular addition of $CaCl_2$ in rabbit ventricular myocytes. Ten consecutive APs were recorded at a frequency of 5 Hz with a CL of 7 s. (A, B, C, D and E) show representative traces from the groups subjected to control, 3.6 mmol/L $CaCl_2$, 3.6 mmol/L $CaCl_2$ and 100 μmol/L barbaloin, 3.6 mmol/L $CaCl_2$ and 200 μmol/L barbaloin and wash-out treatment, respectively. F. Incidence of DADs in the control group, in the presence of 3.6 mmol/L $CaCl_2$ alone, after the addition of 100 μmol/L barbaloin and 200 μmol/L barbaloin and in the wash-out group (n=9. $^{**}P$<0.01 *vs* control. $^{\#\#}P$<0.01 *vs* 3.6 mmol/L $CaCl_2$. $^{\&\&}P$<0.01 *vs* 100 μmol/L barbaloin. $^{\$\$}P$<0.01 *vs* 200 μmol/L barbaloin).

affect the results of studies assessing $I_{Ca.L}$ by using the whole-cell configuration. In our previous study, we have found that $I_{Ca.L}$ tends to be stable for approximately 10 min to 25 min after the whole-cell configuration is established[17]. Therefore, for our studies of $I_{Ca.L}$, we began adding barbaloin 10 min after we established whole-cell configurations, because, at that point, the $I_{Ca.L}$ amplitudes tended to be stable, and we completed the entire experiment within 15 min to prevent the run-down phenomenon from affecting our results. The amplitude of the $I_{Ca.L}$ after inhibition with 100 μmol/L barbaloin recovered after the drug was washed out (Figure 4A). At -5 mV, the voltage at which the $I_{Ca.L}$ density was largest, 100 μmol/L barbaloin decreased the $I_{Ca.L}$ density by 61.7%±3.7%; however, the $I_{Ca.L}$ density returned to 90.5%±8.3% after the drug was washed out (Figure 4B). These results indicated that the effects of barbaloin on $I_{Ca.L}$ were reversible and that the $I_{Ca.L}$ remained stable throughout the experimental period.

Barbaloin (10, 50, 100 and 200 μmol/L) decreased $I_{Ca.L}$ in a concentration-dependent manner (Figure 4C–E). The concentration-response curves for the effects of barbaloin on $I_{Ca.L}$ were plotted and then fitted with the Hill equation to obtain an IC_{50} value of 137.06 μmol/L (Figure 4E).

Barbaloin left-shifted the $I_{Ca.L}$ steady-state inactivation but had no significant effect on the $I_{Ca.L}$ steady-state activation (Figure 4F and 4G). The $V_{1/2}$ for the $I_{Ca.L}$ steady-state inactivation was shifted from -26.90±0.17 mV in the control group to -29.70±0.20 mV in the 200 μmol/L barbaloin-treated group (n=8, P<0.05 *vs* control), and the corresponding k value was shifted from 5.37±0.17 to 5.32±0.19 (n=8, P>0.05 *vs* control). However, in the absence and presence of 200 μmol/L barbal-

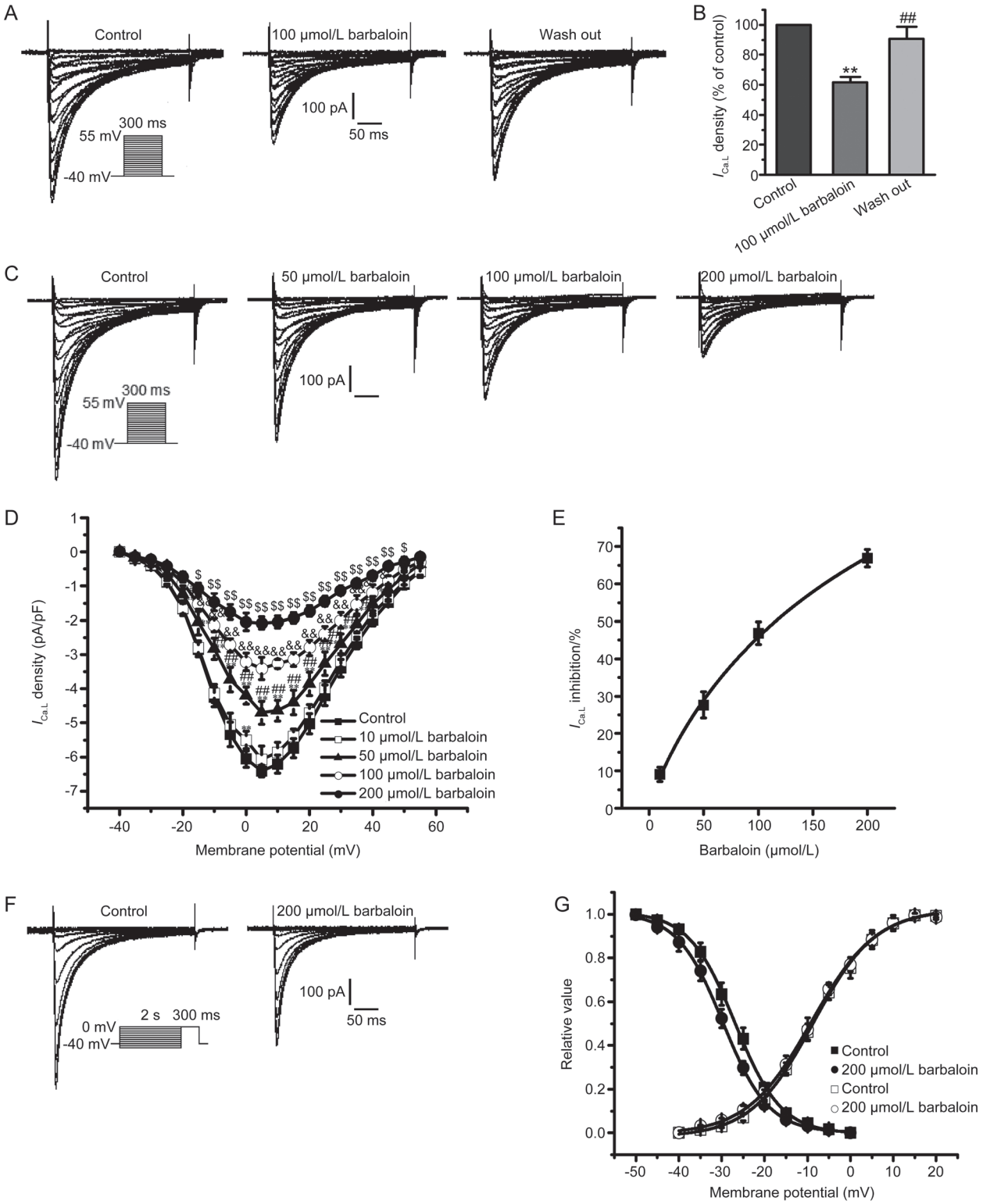

Figure 4. Effects of barbaloin on L-type calcium current ($I_{Ca.L}$) in rabbit ventricular myocytes. (A) Representative traces showing that barbaloin exerted reversible inhibitory effects on $I_{Ca.L}$. (B) The bar graphs show the mean $I_{Ca.L}$ percentage values for the control, 100 μmol/L barbaloin-treated and wash-out groups (n=8. $^{**}P$<0.01 *vs* control. $^{\#\#}P$<0.01 *vs* 100 μmol/L barbaloin). (C) Representative $I_{Ca.L}$ traces from the control and 50, 100 and 200 μmol/L barbaloin-treated groups. (D) $I_{Ca.L}$ current-voltage (I–V) relationships in the control and 10, 50, 100 and 200 μmol/L barbaloin-treated groups (n=8. $^{*}P$<0.05, $^{**}P$<0.01 *vs* control. $^{\#}P$<0.05, $^{\#\#}P$<0.01 *vs* 10 μmol/L barbaloin. $^{\&}P$<0.05, $^{\&\&}P$<0.01 *vs* 50 μmol/L barbaloin. $^{\$}P$<0.05, $^{\$\$}P$<0.01 *vs* 100 μmol/L barbaloin). (E) The concentration-response relationship curve for the effects of barbaloin on $I_{Ca.L}$, fitted to the Hill equation. (F) Representative traces for $I_{Ca.L}$ steady-state inactivation in the control and 200 μmol/L-treated barbaloin groups. (G) Curves for $I_{Ca.L}$ steady-state activation and inactivation before (control) and after the administration of 200 μmol/L barbaloin, fitted to the Boltzmann equation.

oin, the $V_{1/2}$ values for steady-state activation were -8.71±0.28 mV and -9.04±0.27 mV (n=8, P>0.05 *vs* control), respectively, and the corresponding k values were 7.27±0.29 and 7.53±0.28 (n=8, P>0.05 *vs* control).

Effects of barbaloin and TTX on $I_{Na.L}$

$I_{Na.L}$ is generally known as a TTX-sensitive current that is almost completely blocked by 4 μmol/L TTX[16]. The amplitude of the current enhanced by 10 nmol/L ATX II was decreased to almost zero after the administration of 4 μmol/L TTX (Figure 5A). The $I_{Na.L}$ density was increased from -0.32±0.02 pA/pF to -1.45±0.10 pA/pF by 10 nmol/L ATX II (n=8, P<0.01 *vs* control). The administration of 4 μmol/L TTX decreased the current density from -1.45±0.10 to -0.06±0.01 pA/pF (n=8, P<0.01 *vs* control and 10 nmol/L ATX II). These results suggested that the inward current recorded in the control and ATX II-treated groups was $I_{Na.L}$.

After we identified $I_{Na.L}$, we performed experiments to explore the effects of barbaloin on $I_{Na.L}$. We found that 200 μmol/L barbaloin had no significant effect on the amplitude of $I_{Na.L}$ (Figure 5C). However, barbaloin significantly attenuated the amplitude of the $I_{Na.L}$ enhanced by ATX II (Figure 5D, 5E and 5G). Specifically, we found that 100 and 200 μmol/L barbaloin decreased $I_{Na.L}$ in the ATX II-treated group by 36.6%±3.3% and 71.8%±6.5%, respectively (n=8, P<0.01 *vs* 100 μmol/L barbaloin). Moreover, the inhibitory effects of barbaloin on the ATX II-increased $I_{Na.L}$ were reversible (Figure 5B and 5F).

Effects of barbaloin on $I_{Na.P}$

The inhibitory effect of barbaloin on $I_{Na.P}$ was concentration dependent (Figure 6C–E). Barbaloin did not exert significant inhibitory effects on $I_{Na.P}$ at the concentration of 10 μmol/L (Figure 6D). However, barbaloin gradually suppressed $I_{Na.P}$ when its concentration was sequentially increased to 100, 400 and 800 μmol/L (Figure 6C and 6D). The inhibitory effects of 10, 100, 400 and 800 μmol/L barbaloin on $I_{Na.P}$ at -35 mV were fitted with the Hill equation, and the IC_{50} value was 559.80 μmol/L (Figure 6E). Moreover, the inhibitory effects of barbaloin on $I_{Na.P}$ were reversible (Figure 6A and 6B).

Barbaloin exerted different effects on $I_{Na.P}$ steady-state inactivation and steady-state activation (Figure 6F and 6G). Specifically, 200 μmol/L barbaloin increased the $V_{1/2}$ for $I_{Na.P}$ steady-state inactivation from -78.00±0.33 mV to -94.12±0.77 mV (n=8, P<0.01 *vs* control). The corresponding k values were 12.28±0.44 and 12.29±0.55 in the control and 200 μmol/L barbaloin-treated groups, respectively (n=8, P>0.05 *vs* control). However, barbaloin had no significant effect on $I_{Na.P}$ steady-state activation before or after the administration of 200 μmol/L barbaloin, because the $V_{1/2}$ values for $I_{Na.P}$ were -45.83±0.30 mV and -45.35±0.30 mV, respectively (n=8, P>0.05 *vs* control), and the k values were 3.83±0.27 and 4.01±0.27, respectively (n=8, P>0.05 *vs* control).

Effects of barbaloin on I_{K1} and I_{Kr}

I_{Kr} is the rapid component of the delayed rectifier K^+ current, which, in the present study, was measured as a tail current ($I_{Kr\text{-}tail}$) that was recorded during the period in which the cell membrane repolarized to the holding potential. Barbaloin did not exert significant effects on $I_{Kr\text{-}tail}$ at the concentrations of 100 or 800 μmol/L (Figure 7A, 7B). In agreement with these findings, we found that I_{K1} was almost unchanged after the administration of 100 and 800 μmol/L barbaloin (Figure 7C, 7D).

Effects of barbaloin on aconitine-induced ventricular arrhythmias in Langendorff-perfused rabbit hearts

Aconitine is an alkaloid derived from herbal aconitum plants that has been reported to cause arrhythmia[18-20]. In the present study, 100 nmol/L aconitine led to an accelerated heart rate and caused ventricular tachycardia (VT) and ventricular fibrillation (VF) in Langendorff-perfused rabbit hearts (Figure 8A, 8B and 8C). Barbaloin (200 μmol/L) decreased the heart rates in both the barbaloin-treated group and the barbaloin and aconitine co-treatment group (Figure 8B and 8C). Moreover, 200 μmol/L barbaloin effectively delayed the onset time and decreased the incidence of VT and VF induced by 100 nmol/L aconitine (Figure 8A, 8B, 8C and 8D).

Discussion

Barbaloin is a major component of the herbal plant aloe and has been reported to have multiple pharmacological effects. However, the effects of barbaloin on cardiac electrophysiology had been unknown. To the best of our knowledge, this study is the first to explore the effects of barbaloin on APs, multiple transmembrane ionic currents in cardiomyocytes and Langendorff-perfused rabbit hearts. In the present study, we found that barbaloin has multiple effects on ventricular myocytes. First, barbaloin shortened the APD_{50}, and the APD_{90}, decreased the V_{max} and attenuated the APD RRD. Second, barbaloin eliminated EADs and DADs. Third, barbaloin significantly inhibited $I_{Ca,L}$, $I_{Na.P}$ and ATX II-induced $I_{Na.L}$ enhancements. Fourth, barbaloin exerted no significant effects on I_{K1} or I_{Kr}. Finally, barbaloin inhibited the aconitine-induced ventricular arrhythmias in Langendorff-perfused rabbit hearts.

It is well known that APs are generated by transmembrane ionic currents. Therefore, AP alternations may be attributed to changes in different transmembrane ionic currents. In the present study, barbaloin had distinct effects on different AP parameters. Barbaloin did not exert significant effects on the RMP at the above-mentioned experimental concentrations, a finding supported by our observation that I_{K1} was unchanged. Although barbaloin significantly decreased $I_{Na.P}$, the concentrations of the drug that were administered herein were higher than those that exhibited effects on APs. This finding accounts for the slight decrease in V_{max} after barbaloin treatment. In contrast, barbaloin significantly shortened the APD_{50} and APD_{90} and decreased the APD_{90} to almost the same extent as it decreased the APD_{50}. Moreover, the APD_{50}/APD_{90} ratios were almost equal in the absence and presence of barbaloin, thus indicating that barbaloin affects the plateau phase of the AP. This phenomenon was elucidated further in subsequent

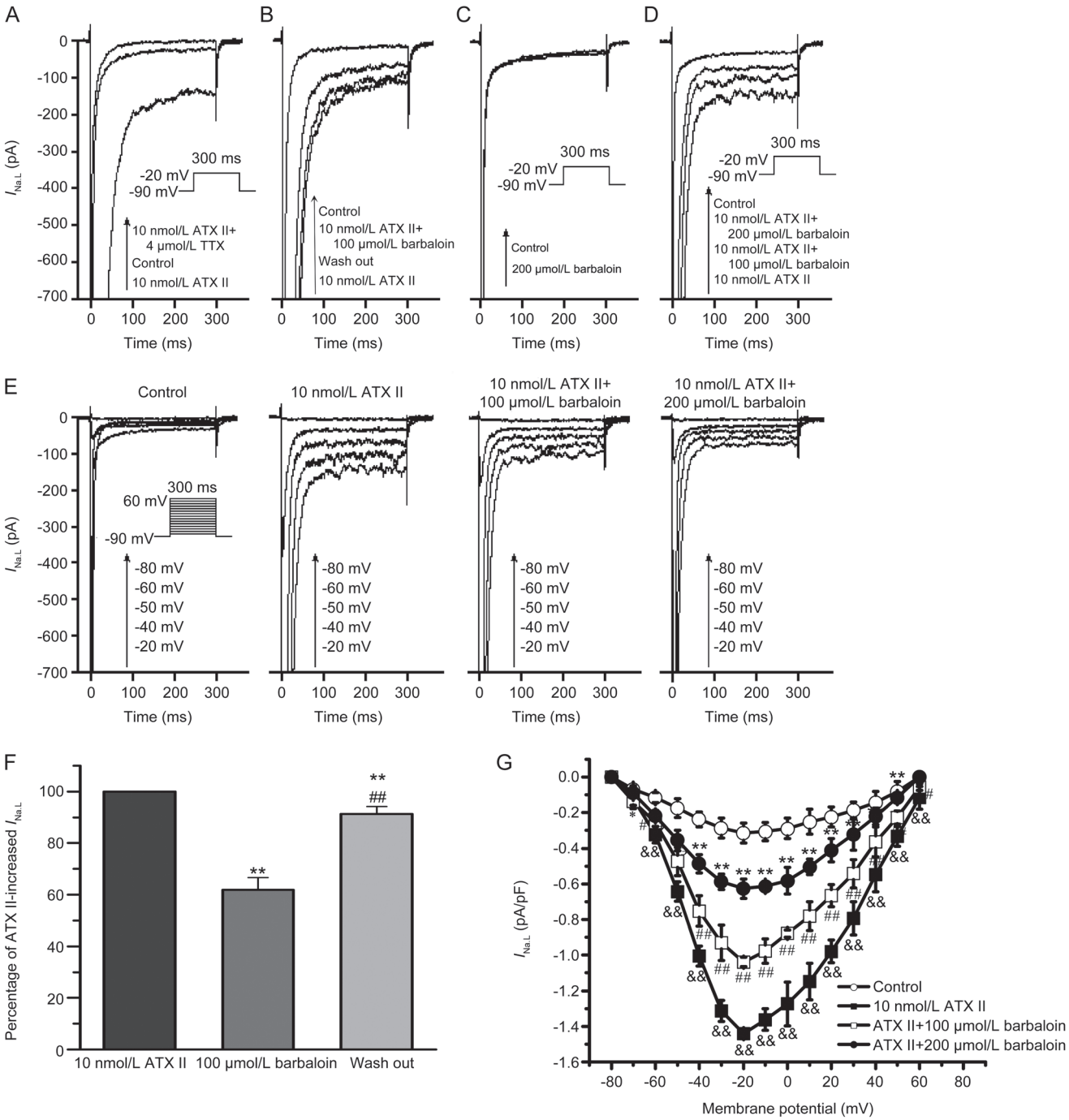

Figure 5. Effects of barbaloin on ATX II-induced late sodium current ($I_{Na.L}$) enhancements and under normal conditions in rabbit ventricular myocytes. (A) Representative single traces of the effects of 4 μmol/L TTX on ATX II-induced $I_{Na.L}$ enhancement. (B) Representative single traces showing that barbaloin exerted reversible inhibitory effects on ATX II-induced $I_{Na.L}$ enhancement. (C) Representative single traces of the effects of 200 μmol/L barbaloin on $I_{Na.L}$ under normal conditions. (D) Single traces of the effects of barbaloin on ATX II-induced $I_{Na.L}$ enhancements at a membrane potential of -20 mV. (E) Representative traces of the effects of barbaloin on ATX II-induced $I_{Na.L}$ enhancements at membrane potentials of -80, -60, -50, -40 and -20 mV. (F) Bar graphs showing the mean ATX II-increased $I_{Na.L}$ percentage values for the control, 100 μmol/L barbaloin-treated and wash-out groups (n=10. $^{**}P$<0.01 *vs* control. $^{\#\#}P$<0.01 *vs* 100 μmol/L barbaloin). (G) The *I-V* relationship for the effects of barbaloin on ATX II-induced $I_{Na.L}$ enhancement (n=8. $^{*}P$<0.05, $^{**}P$<0.01 *vs* control. $^{\#}P$<0.05, $^{\#\#}P$<0.01 *vs* 10 nmol/L ATX II. $^{\&}P$<0.05, $^{\&\&}P$<0.01 *vs* 100 μmol/L barbaloin).

experiments. Barbaloin significantly decreased $I_{Ca.L}$, the major inward current of the plateau phase of the AP, but did not have significant effects on I_{K1} or I_{Kr}. Thus, the inhibitory effects of barbaloin on $I_{Ca.L}$ appeared to be the main contributor to the APD-shortening effects of the drug.

APD RRD indicates that the APD shortens as the heart rate

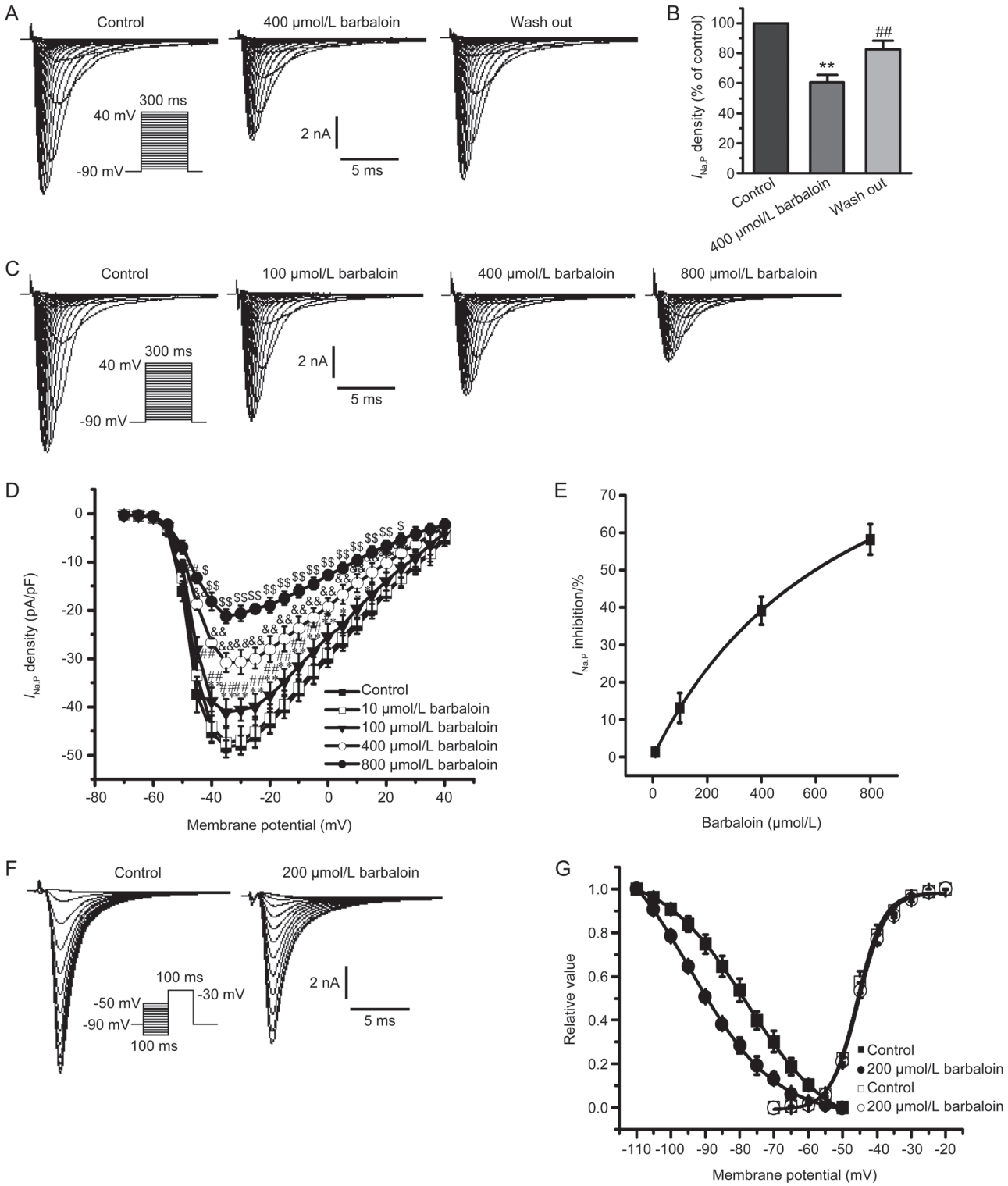

Figure 6. Effects of barbaloin on peak sodium current ($I_{Na.P}$) in rabbit ventricular myocytes. (A) Representative traces showing that barbaloin exerted reversible inhibitory effects on $I_{Na.P}$. (B) Bar graphs showing the mean $I_{Na.P}$ percentage values for the control, 400 μmol/L barbaloin-treated and wash-out groups (n=10. $^{*}P$<0.05, $^{**}P$<0.01 *vs* control. $^{\#\#}P$<0.01 *vs* 400 μmol/L barbaloin). (C) Representative $I_{Na.P}$ traces from the control and 100, 400 and 800 μmol/L barbaloin-treated groups. (D) *I-V* relationships for $I_{Na.P}$ in the control and 10, 100, 400 and 800 μmol/L barbaloin-treated groups (n=8. $^{*}P$<0.05, $^{**}P$<0.01 *vs* control. $^{\#}P$<0.05, $^{\#\#}P$<0.01 *vs* 10 μmol/L barbaloin. $^{\&}P$<0.05, $^{\&\&}P$<0.01 *vs* 100 μmol/L barbaloin. $^{\$}P$<0.05, $^{\$\$}P$<0.01 *vs* 400 μmol/L barbaloin). (E) The concentration-response relationship curve for the effects of barbaloin on $I_{Na.P}$, fitted to the Hill equation. (F) Representative traces of $I_{Na.P}$ steady-state inactivation in the control and 200 μmol/L barbaloin-treated groups. (G) Curves for $I_{Na.P}$ steady-state activation and inactivation before (control) and after the administration of 200 μmol/L barbaloin, fitted to the Boltzmann equation.

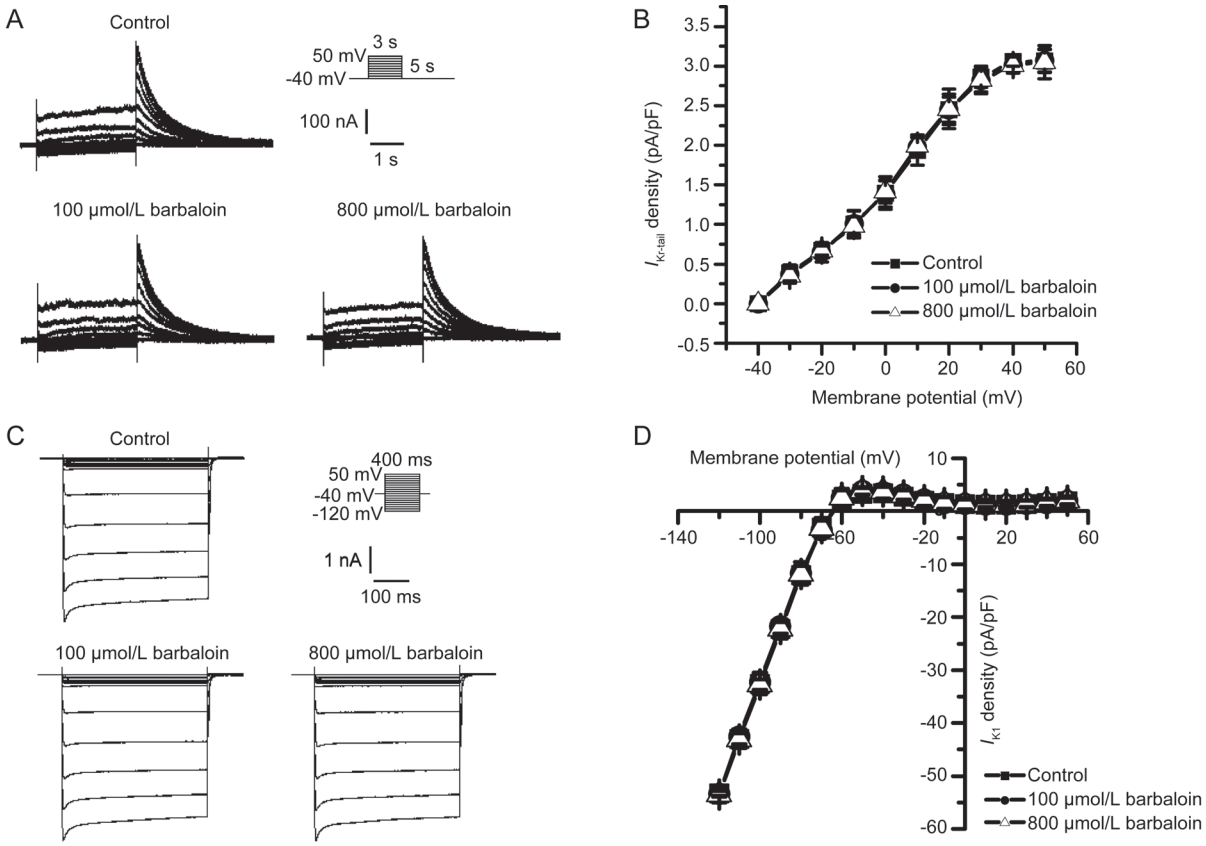

Figure 7. Barbaloin had similar effects on inward rectifier potassium current (I_{K1}) and rapidly activated delayed rectifier potassium current (I_{Kr}) in rabbit ventricular myocytes. (A) Representative I_{Kr} traces from the control and 100 and 800 μmol/L barbaloin-treated groups. (B) *I–V* relationships for $I_{Kr\text{-}tail}$ in the control and 100 and 800 μmol/L barbaloin-treated groups (n=8, P>0.05 for both 100 and 800 μmol/L barbaloin *vs* control). (C) Representative I_{K1} traces from the control and 100 and 800 μmol/L barbaloin-treated groups. (D) *I–V* relationships for I_{K1} in the control and 100 and 800 μmol/L barbaloin-treated groups (n=8, P>0.05 for both 100 and 800 μmol/L barbaloin *vs* control).

or stimulation frequency increases, and *vice versa*. The transmural dispersion of repolarization (TDR) of the ventricle is determined mainly by the difference in the APD between midmyocardial and endocardial myocytes[21]. In the present study, barbaloin attenuated the APD RRD. When the RRD decreased, the TDR decreased, thus indicating that barbaloin decreases the TDR. The TDR increases in pathological conditions, such as heart failure, thus resulting in ventricular tachyarrhythmias (VTs)[22]. Therefore, our results indicated that barbaloin attenuates VT by decreasing the TDR. Moreover, it has been reported that $I_{Ca.L}$ inhibition significantly decreases the TDR and thus ultimately suppresses VTs[23]. From these findings, we speculate that barbaloin is likely to decrease the TDR by inhibiting $I_{Ca.L}$, thereby attenuating arrhythmias.

EADs play an important role in arrhythmogenesis. Increases in $I_{Na.L}$ have been reported to be important with respect to the occurrence of EADs[15, 24]. Another important inward current constituting the plateau phase of the AP, the $I_{Na.L}$, has been documented to be enhanced by various pathological factors, such as heart failure, hypoxia/ischemia and oxidative stress, and to lead to APD prolongation[25-27]. APD prolongation provides sufficient time for $I_{Ca.L}$ re-activation, thus resulting in EADs [28]. In the present study, ATX II, an $I_{Na.L}$ opener, was administered to induce EADs. Our results demonstrated that administering ATX II facilitated the occurrence of EADs and APD prolongation, and these findings were consistent with those of previous studies[15, 24]. Barbaloin eliminated these ATX II-induced EADs and significantly attenuated the effects of ATX II on the APD. Furthermore, barbaloin also significantly inhibited ATX II-induced $I_{Na.L}$ enhancement. These findings indicated that barbaloin eliminates ATX II-induced EADs by inhibiting $I_{Na.L}$ enhancement; hence, these currents may be a promising target for the treatment of arrhythmias[29].

DADs, an important cause of arrhythmias, occur under Ca^{2+} overload conditions in cardiomyocytes. Ca^{2+} overload drives the reverse Na^+/Ca^{2+} exchange current (I_{NCX}), which functions as an inward current characterized by the simultaneous entry of 3 Na^+ and exit of 1 Ca^{2+}, and ultimately leads to the development of a transient inward current I_{Ti} that is known tocause DADs[30]. Katra *et al* have reported that rapid pacing contributes to spontaneous calcium release (SCR) from the sarcoplasmic reticulum[31], thus indicating that rapid pacing is an effective means of increasing cytoplasmic Ca^{2+} levels. However, increases in $[Ca^{2+}]_o$ are also known to be one of the contributors to enhancements of $I_{Ca.L}$; as such, increases in $[Ca^{2+}]_o$ lead to subsequent increases in Ca^{2+} influx and Ca^{2+} overload.

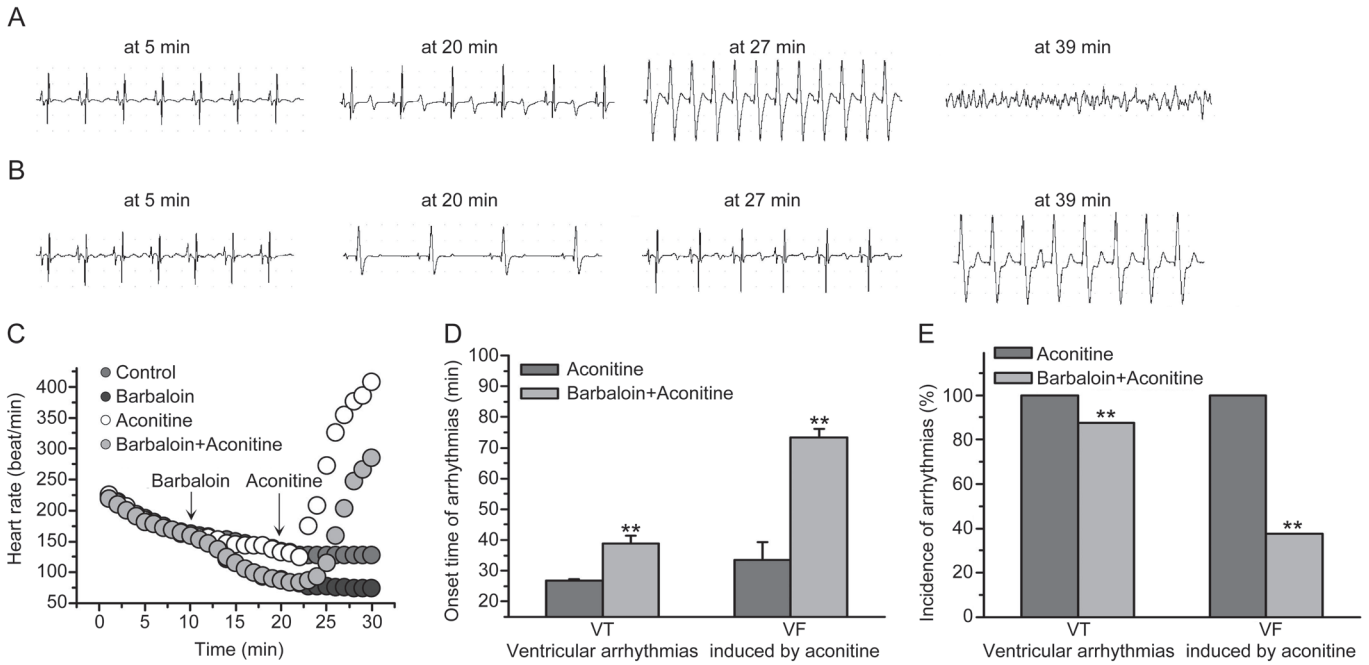

Figure 8. Effects of barbaloin on aconitine-induced ventricular arrhythmias in Langendorff-perfused rabbit hearts. (A) Representative ECG traces at onset time in the aconitine-treated group. (B) Representative ECG traces at the same time as A in the barbaloin and aconitine co-treatment group. (C) The heart rates of the Langendorff-perfused rabbit hearts for the first 30 min of recording time in four different groups. The arrows indicate the time when barbaloin or aconitine was added to the perfusate. (D) The onset time of aconitine-induced ventricular arrhythmias in the aconitine-treated and barbaloin and aconitine co-treatment groups (n=8. $^{**}P$<0.01 *vs* aconitine group). (E) The incidence of aconitine-induced ventricular arrhythmias in the aconitine-treated and barbaloin and aconitine co-treatment groups (n=8, $^{**}P$<0.01 *vs* aconitine group).

In the present study, we administered increased $[Ca^{2+}]_o$ and rapid pacing to induce DADs, and this endeavor was successful. Barbaloin eliminated these DADs. $I_{Ca.L}$ inhibition, which directly decreases Ca^{2+} influx, appeared to be responsible for the antiarrhythmic effects of barbaloin.

The major source of intracellular Ca^{2+} ($[Ca^{2+}]_i$), $I_{Ca.L}$ contributes greatly to Ca^{2+} influx and maintaining $[Ca^{2+}]_i$ homeostasis. Ca^{2+} participates in many important cellular activities, such as intracellular signaling pathways and cardiac excitation-contraction-coupling[32, 33]; thus, $[Ca^{2+}]_i$ homeostasis is of great importance for the regulation of vital functions. The results of several reports have indicated that many pathological conditions cause intracellular Ca^{2+} overload and thereby lead to arrhythmias[18, 34-37]. In the present study, barbaloin decreased the amplitude of $I_{Ca.L}$ in a concentration-dependent manner. When the amplitude of $I_{Ca.L}$ decreases, the number of open calcium channels decreases, thus decreasing Ca^{2+} flow into the cell. Additionally, barbaloin accelerated $I_{Ca.L}$ steady-state inactivation and thereby decreased the quantity of Ca^{2+} flowing into the cell during the inactivation process. These findings indicated that barbaloin effectively decreases $[Ca^{2+}]_i$ and subsequently relieves intracellular Ca^{2+} overload and may thus potently suppress Ca^{2+} overload-induced arrhythmias.

In our previous study, we have found that increases in $I_{Na.L}$ contribute to the development of intracellular Ca^{2+} overload by enhancing I_{NCX}[25, 38]. Another study has demonstrated that elevated $[Ca^{2+}]_i$ activates the CaMK II and PKC pathways, and ultimately increases $I_{Na.L}$ and results in the formation of a vicious cycle[39]. Thus, inhibiting pathological increases in $I_{Na.L}$ is of great importance with respect to attenuating intracellular Ca^{2+} overload and ultimately alleviating arrhythmias. In this study, barbaloin exerted significant inhibitory effects on ATX II-induced increases in $I_{Na.L}$, thus suggesting that the drug also attenuates intracellular Ca^{2+} overload and protects the heart from arrhythmia through this mechanism in addition to those mentioned above.

$I_{Na.P}$ is responsible for the upstroke of the AP in individual cardiomyocytes and determines myocardial excitability[40]. When the amplitude of $I_{Na.P}$ decreases, the V_{max} of the AP decreases, thereby contributing to decreases in myocardial excitability. It has been reported that increases in myocardial excitability result in tachyarrhythmias, such as ventricular fibrillation[41]. Thus, decreasing cardiac myocyte excitability is an effective means of attenuating tachyarrhythmias. In the present study, barbaloin had significant inhibitory effects on $I_{Na.P,}$ thus indicating that barbaloin is effective at decreasing the numbers of open sodium channels and consequently decreasing the Na^+ influx and accordingly the cardiac myocyte excitability. Moreover, barbaloin shifted the $I_{Na.P}$ steady-state inactivation to a more negative potential and accelerated the $I_{Na.P}$ inactivation process, thus decreasingthe Na^+ influx during the inactivation process and the cardiac myocyte excitability. Together, the above findings indicated that barbaloin decreases cardiac myocyte excitability by inhibiting $I_{Na.P}$ and

thereby exerting its antiarrhythmic effects.

Although barbaloin had inhibitory effects on multiple ion channels, it exerted no effects on I_{Kr} even when it was administered at a much higher concentration than those used in other experiments. A variety of clinical drugs are likely to cause arrhythmias by inhibiting I_{Kr}[42, 43]. Thus, determining the potency of a particular drug's ability to antagonize I_{Kr} is important when assessing the proarrhythmic effects of new drugs. The above findings regarding the effects of barbaloin on I_{Kr} support the safety of this drug.

It is well known that a decreased heart rate contributes to a lower tendency to develop tachyarrhythmias[44]. Barbaloin decreased the heart rate in the Langendorff-perfused hearts, thus indicating that barbaloin has the potential to rescue tachyarrhythmias. Aconitine has been reported to increase the $I_{Na.P}$, thereby inducing intracellular Na^+ accumulation and thus leading to intracellular Ca^{2+} overload[19]. Additionally, aconitine increases the $I_{Ca.L}$ and consequently aggravates the intracellular Ca^{2+} overload and ultimately causes arrhythmias[19, 45]. In the present study, barbaloin was effective in delaying the onset time and the incidence of aconitine-induced ventricular arrhythmias. The above findings indicate that the inhibitory effects of barbaloin on $I_{Na.P}$, $I_{Na.L}$ and $I_{Ca.L}$, which can relieve intracellular Ca^{2+} overload, may underlie its antiarrhythmic mechanisms.

In conclusion, barbaloin is an effective antiarrhythmic component extracted from aloe, and its ability to inhibit $I_{Ca.L}$, $I_{Na.P}$ and ATX II-enhanced $I_{Na.L}$ appear to underlie its antiarrhythmic effects. Moreover, barbaloin exerted no effects on I_{Kr}, thus suggesting that it is a highly safe drug. Together, our findings indicate that barbaloin has potential as an antiarrhythmic drug.

Acknowledgments

This research did not receive any specific grant from funding agencies in the public, commercial, or not-for-profit sectors.

Author contribution

Zhen-zhen CAO, Jie HAO and Ji-hua MA designed the research. Zhen-zhen CAO, You-jia TIAN, Pei-hua ZHANG and Zhi-pei LIU performed the research. Wan-zhen JIANG, Meng-liu ZENG, and Pei-pei ZHANG analyzed the data. Zhen-zhen CAO, You-jia TIAN and Jie HAO wrote the paper. Ji-hua MA supervised the research.

References

1 Song XF, Chen XD. Advances in the research of promotion effect of Aloe vera on wound healing and its clinical use. Zhonghua Shao Shang Za Zhi 2016; 32: 634–37.
2 Eshun K, He Q. Aloe vera: a valuable ingredient for the food, pharmaceutical and cosmetic industries-a review. Crit Rev Food Sci Nutr 2004; 44: 91–6.
3 Rajkumar V, Verma AK, Patra G, Pradhan S, Biswas S, Chauhan P, *et al.* Quality and acceptability of meat nuggets with fresh aloe vera gel. Asian-Australas J Anim Sci 2016; 29: 702–8.
4 Patel DK, Patel K, Tahilyani V. Barbaloin: a concise report of its pharmacological and analytical aspects. Asian Pac J Trop Biomed 2012; 2: 835–8.
5 Silva MA, Trevisan G, Hoffmeister C, Rossato MF, Boligon AA, Walker CI, *et al.* Anti-inflammatory and antioxidant effects of Aloe saponaria Haw in a model of UVB-induced paw sunburn in rats. J Photochem Photobiol B 2014; 133: 47–54.
6 Alves DS, Perez-Fons L, Estepa A, Micol V. Membrane-related effects underlying the biological activity of the anthraquinones emodin and barbaloin. Biochem Pharmacol 2004; 68: 549–61.
7 Oumer A, Bisrat D, Mazumder A, Asres K. A new antimicrobial anthrone from the leaf latex of Aloe trichosantha. Nat Prod Commun 2014; 9: 949–52.
8 El-Shemy HA, Aboul-Soud MA, Nassr-Allah AA, Aboul-Enein KM, Kabash A, Yagi A. Antitumor properties and modulation of antioxidant enzymes' activity by Aloe vera leaf active principles isolated via supercritical carbon dioxide extraction. Curr Med Chem 2010; 17: 129–38.
9 Beppu H, Koike T, Shimpo K, Chihara T, Hoshino M, Ida C, *et al.* Radical-scavenging effects of Aloe arborescens Miller on prevention of pancreatic islet B-cell destruction in rats. J Ethnopharmacol 2003; 89: 37–45.
10 Lam RY, Woo AY, Leung PS, Cheng CH. Antioxidant actions of phenolic compounds found in dietary plants on low-density lipoprotein and erythrocytes *in vitro*. J Am Coll Nutr 2007; 26: 233–42.
11 Pimentel M, Zimerman A, Chemello D, Giaretta V, Andrades M, Silvello D, *et al.* Predictors of serious arrhythmic events in patients with nonischemic heart failure. J Int Cardiovasc Electrophysiol 2017; 48: 131–9.
12 Marsman RF, Tan HL, Bezzina CR. Genetics of sudden cardiac death caused by ventricular arrhythmias. Nat Rev Cardiol 2014; 11: 96–111.
13 Tanaka H, Matsuyama TA, Takamatsu T. Towards an integrated understanding of cardiac arrhythmogenesis–growing roles of experimental pathology. Pathol Int 2017; 67: 8–16.
14 Nerbonne JM, Kass RS. Molecular physiology of cardiac repolarization. Physiol Rev 2005; 85: 1205–53.
15 Shryock JC, Song Y, Rajamani S, Antzelevitch C, Belardinelli L. The arrhythmogenic consequences of increasing late I_{Na} in the cardiomyocyte. Cardiovasc Res 2013; 99: 600–11.
16 Wang C, Wang LL, Zhang C, Cao ZZ, Luo AT, Zhang PH, *et al*. Tolterodine reduces veratridine-augmented late I_{Na}, reverse-I_{NCX} and early afterdepolarizations in isolated rabbit ventricular myocytes. Acta Pharmacol Sin 2016; 37: 1432–41.
17 Ren Z, Ma J, Zhang P, Luo A, Zhang S, Kong L, *et al*. The effect of ligustrazine on L-type calcium current, calcium transient and contractility in rabbit ventricular myocytes. J Ethnopharmacol 2012; 144: 555–61.
18 Sun GB, Sun H, Meng XB, Hu J, Zhang Q, Liu B, *et al.* Aconitine-induced Ca^{2+} overload causes arrhythmia and triggers apoptosis through p38 MAPK signaling pathway in rats. Toxicol Appl Pharmacol 2014; 279: 8–22.
19 Zhao Z, Yin Y, Wu H, Jiang M, Lou J, Bai G, *et al.* Arctigenin, a potential anti-arrhythmic agent, inhibits aconitine-induced arrhythmia by regulating multi-ion channels. Cell Physiol Biochem 2013; 32: 1342–53.
20 Bai DL, Chen WZ, Bo YX, Dong YL, Kang AL, Sun WK, *et al*. Discovery of *N*-(3,5-*bis*(1-pyrrolidylmethyl)-4-hydroxybenzyl)-4-methoxybenzenesulfamide (sulcardine) as a novel anti-arrhythmic agent. Acta Pharmacol Sin 2012; 33: 1176–86.
21 Xu T, Wang H, Zhang JY, Zhang Y, Zhang R, Jiang LQ, *et al.* Effects of mid-myocardial pacing on transmural dispersion of repolarization and arrhythmogenesis. Europace 2012; 14: 1363–8.

22 Akar FG, Rosenbaum DS. Transmural electrophysiological heterogeneities underlying arrhythmogenesis in heart failure. Circ Res 2003; 93: 638–45.
23 Milberg P, Fink M, Pott C, Frommeyer G, Biertz J, Osada N, *et al.* Blockade of I_{Ca} suppresses early afterdepolarizations and reduces transmural dispersion of repolarization in a whole heart model of chronic heart failure. Br J Pharmacol 2012; 166: 557–68.
24 Jones DK, Ruben PC. Proton modulation of cardiac I_{Na}: a potential arrhythmogenic trigger. Handb Exp Pharmacol 2014; 221: 169–81.
25 Tang Q, Ma J, Zhang P, Wan W, Kong L, Wu L. Persistent sodium current and Na^+/H^+ exchange contributes to the augmentation of the reverse Na^+/Ca^{2+} exchange during hypoxia or acute ischemia in ventricular myocytes. Pflugers Arch 2012; 463: 513–22.
26 Undrovinas A, Maltsev VA. Late sodium current is a new therapeutic target to improve contractility and rhythm in failing heart. Cardiovasc Hematol Agents Med Chem 2008; 6: 348–59.
27 Ward CA, Giles WR. Ionic mechanism of the effects of hydrogen peroxide in rat ventricular myocytes. J Physiol 1997; 500: 631–42.
28 Xie LH, Chen F, Karagueuzian HS, Weiss JN. Oxidative-stress-induced afterdepolarizations and calmodulin kinase II signaling. Circ Res 2009; 104: 79–86.
29 Du YM, Xia CK, Zhao N, Dong Q, Lei M, Xia JH. 18beta-Glycyrrhetinic acid preferentially blocks late Na current generated by DeltaKPQ Nav1.5 channels. Acta Pharmacol Sin 2012; 33: 752–60.
30 Katra RP, Laurita KR. Cellular mechanism of calcium-mediated triggered activity in the heart. Circ Res 2005; 96: 535–42.
31 Fedida D, Noble D, Rankin AC, Spindler AJ. The arrhythmogenic transient inward current iTI and related contraction in isolated guinea-pig ventricular myocytes. J Physiol 1987; 392: 523–42.
32 Santonastasi M, Wehrens XH. Ryanodine receptors as pharmacological targets for heart disease. Acta Pharmacol Sin 2007; 28: 937–44.
33 Jiang QS, Huang XN, Yang GZ, Jiang XY, Zhou QX. Inhibitory effect of ginsenoside Rb1 on calcineurin signal pathway in cardiomyocyte hypertrophy induced by prostaglandin F2alpha. Acta Pharmacol Sin 2007; 28: 1149–54.
34 Yin G, Hassan F, Haroun AR, Murphy LL, Crotti L, Schwartz PJ, *et al*. Arrhythmogenic calmodulin mutations disrupt intracellular cardiomyocyte Ca^{2+} regulation by distinct mechanisms. J Am Heart Assoc 2014; 3: e000996.
35 Sedej S, Heinzel FR, Walther S, Dybkova N, Wakula P, Groborz J, *et al.* Na^+-dependent SR Ca^{2+} overload induces arrhythmogenic events in mouse cardiomyocytes with a human CPVT mutation. Cardiovasc Res 2010; 87: 50–9.
36 Rickover O, Zinman T, Kaplan D, Shainberg A. Exogenous nitric oxide triggers classic ischemic preconditioning by preventing intracellular Ca^{2+} overload in cardiomyocytes. Cell Calcium 2008; 43: 324–33.
37 Zhang X, Ai X, Nakayama H, Chen B, Harris DM, Tang M, *et al*. Persistent increases in Ca^{2+} influx through Cav1.2 shortens action potential and causes Ca^{2+} overload-induced afterdepolarizations and arrhythmias. Basic Res Cardiol 2016; 111: 4.
38 Luo AT, Cao ZZ, Xiang Y, Zhang S, Qian CP, Fu C, *et al.* Ketamine attenuates the Na^+-dependent Ca^{2+} overload in rabbit ventricular myocytes *in vitro* by inhibiting late Na^+ and L-type Ca^{2+} currents. Acta Pharmacol Sin 2015; 36: 1327–36.
39 Ma J, Luo A, Wu L, Wan W, Zhang P, Ren Z, *et al.* Calmodulin kinase II and protein kinase C mediate the effect of increased intracellular calcium to augment late sodium current in rabbit ventricular myocytes. Am J Physiol Cell Physiol 2012; 302: C1141–51.
40 Amin AS, Tan HL, Wilde AA. Cardiac ion channels in health and disease. Heart Rhythm 2010; 7: 117–26.
41 Ten Tusscher KH, Hren R, Panfilov AV. Organization of ventricular fibrillation in the human heart. Circ Res 2007; 100: e87–101.
42 Cubeddu LX. QT prolongation and fatal arrhythmias: a review of clinical implications and effects of drugs. Am J Ther 2003; 10: 452–7.
43 Han SN, Jing Y, Yang LL, Zhang Z, Zhang LR. Propofol inhibits hERG K^+ channels and enhances the inhibition effects on its mutations in HEK293 cells. Eur J Pharmacol 2016; 791: 168–78.
44 Osadchii OE. Reduced intrinsic heart rate is associated with reduced arrhythmic susceptibility in guinea-pig heart. Scand Cardiovasc J 2014; 48: 357–67.
45 Liu Y, Sun HL, Li DL, Wang LY, Gao Y, Wang YP, *et al.* Choline produces antiarrhythmic actions in animal models by cardiac M3 receptors: improvement of intracellular Ca^{2+} handling as a common mechanism. Can J Physiol Pharmacol 2008; 86: 860–5.